C-CORE Publication No. 90-1

The American Society of Mechanical Engineers

Reprinted From
Proceedings of The Ninth International Conference of Offshore Mechanics and Arctic Engineering
Editors: O. A. Ayorinde, N. K. Sinha, and D. S. Sodhi
Book No. I0296F — 1990

WAVE-INDUCED BERGY BIT MOTION NEAR A FLOATING OIL PRODUCTION PLATFORM

L. M. Mak
Faculty of Engineering and Applied Science
Memorial University of Newfoundland
St. John's, Newfoundland, Canada

J. H. Lever
U.S. Army Cold Regions Research and Engineering Laboratory
Hanover, New Hampshire

M. J. Hinchey
Faculty of Engineering and Applied Science
Memorial University of Newfoundland
St. John's Newfoundland, Canada

D. Duthinh
Centre for Cold Ocean Resources Engineering
Memorial University of Newfoundland
St. John's Newfoundland, Canada

ABSTRACT

This paper describes an experimental study at model scale of wave-induced impacts of bergy bits with a floating oil production platform intended for use on the Grand Banks of Newfoundland, Canada. We conducted the tests in the 58 m wave tank at Memorial University using techniques developed in an earlier pilot study but refined in the present program to improve data quality. The objective was to collect and analyze a statistically valid set of bergy bit impact velocities and locations, with a view to providing the design information necessary to ice-strengthen the platform.

We used a JONSWAP wave-energy spectrum to simulate a 10 m irregular sea on the Grand Banks, and we constructed a platform model and cubical models of 1000 tonne and 5000 tonne bergy bits. During the impact tests, a SELSPOT system continuously recorded the 6 degrees-of-freedom of the bergy bit and the platform; by repeating the tests, we collected desired impact statistics. We then used the solid modelling capabilities of a CAD system to recreate the measured model motions. This enabled us to determine the impact locations and compute the impact velocities and kinetic energies. We confirmed the CAD-generated impact sequences using video records, and verified the impact times and locations using output from piezoelectric sensors mounted on the platform.

We conclude from the study that (1) open-water iceberg significant velocities can provide conservative estimates of the significant impact velocities; (2) relative motion between the platform and the iceberg tends, on average, to mitigate impacts; (3) the berg rotational kinetic energy at the time of an impact is a small portion of the translational kinetic energy; (4) the most probable impact location on the platform is the upper corner of the pontoon facing the oncoming waves; (5) wave diffraction from the structure can reduce impact velocities and change iceberg trajectories; and (6) wave diffraction has more influence on the smaller bergy bit, resulting in fewer impacts. The paper compares the impact results obtained for this floating production platform with results obtained previously for a more transparent, exploration-style semi-submersible.

1.0 INTRODUCTION

Bergy bits pose a serious hazard to floating offshore structures. This is because they are difficult to detect [1,2] and can be driven by storm waves to high velocities [3,4,5,6,7]. Even when detected, bergy bits are rather difficult to deflect because they are very unstable [2,8,9]. In view of the hazards associated with bergy bits and the limitations of existing iceberg management methods, ice strengthening of floating platforms at critical locations may be necessary. It may also reduce the loss of valuable operating time if the platform must otherwise move off-station when threatened by ice.

The present knowledge of wave-induced impacts of bergy bits has provided some valuable design information to ice-strengthen structures. In a pilot study for the present work, Lever et al. [10] collected statistics of impact velocities for an exploration-style semi-submersible, which is approximately transparent to waves. They also developed a simple theory for a transparent structure which predicts statistics of impact velocities and kinetic energies using only standard deviations of iceberg velocities in open water. The reasonable agreement between the theoretical and experimental results obtained in the study implies that wave diffraction has little effect on iceberg impact when the platform is approximately transparent. With more robust structures, however, wave diffraction may reduce velocities and change hydrodynamic parameters of the approaching iceberg [11,12,13]. Therefore, ignoring the effect of wave diffraction should give conservative results, perhaps excessively so.

The pilot study clearly indicated that bergy bits in waves may undergo large excursions during impact with a structure. The simulation of such behaviour would require a nonlinear, two-body hydrodynamic model, such as the one being developed by Pawlowski and Wishahy [14,15]. They assume that the ice moves within the structure-modified wave field without disturbing that wave field. They compute the hydrodynamic forces on the instantaneous wetted surface of the ice using potential-flow theory and account for viscous effects empirically. In this way, they model the nonlinear effects of large body excursions (including submergence) and fluid transport in steep waves. However, such models are still in the early stages of development and eventually require validation for impact simulation. We therefore chose to continue our experimental approach.

This paper describes a study carried out to investigate the collision of bergy bits with a semi-submersible platform being considered for production of oil on the Grand Banks. As this platform is capable of processing and storing crude oil, it has larger physical dimensions than the structure investigated in the pilot program. Hence, we anticipated that wave diffraction would have a greater influence than in the previous study.

Because collisions between bergy bits and an offshore structure are random processes, the selection of an iceberg impact design load must be based on risk analysis. To conduct such analyses, we require information on many random factors, including iceberg populations, size distributions, shapes, drift speeds, etc. However, we limited our investigation to the study of berg impact velocities and locations on the platform as a function of berg size and rig orientation. Only parent probability distributions were generated, dealing with velocities and kinetic energies of individual impacts. However, iceberg impact design loads should be based on extremal analysis (see, for example, [16,17]). That is, when predicting the most severe impact expected, designers must consider the number of impacts likely to occur during the lifespan of the structure, including repeated impacts by the same ice mass during a given incursion. In comparison with what is known about impact velocities, very little information exists regarding the number of impacts likely for each iceberg incursion, yet this has a direct effect on the extremal statistics.

The objective was to apply an experimental procedure to collect and analyze statistics of impact velocities and locations on the rig with a view to providing design information necessary to ice strengthen the platform. The experience gained from the previous tests enabled improvements in both the experiment and data analyzing methodology. In addition to the irregular sea impact tests carried out in the pilot program, the present study included regular sea impact tests, investigation of rig motion behaviour and probable impact location, and impact velocity error estimations.

2.0 THE EXPERIMENTAL METHODOLOGY

The Memorial University wave tank has inside dimensions of 58.7 m (length) x 4.57 m (width) x 3.0 m (depth). A hydraulic piston-type generator generates waves at one end of the tank, and a parabolic beach absorbs them at the other end.

We used Froude scaling (at a scale of 1:75) because Lever et al. [18] have shown that fluid viscosity has a significant effect on wave-induced motion of bergy bits only near resonance. Thus, for moderate motions, it can be ignored. The scaling relationships thus are:

$$L_p = \lambda_0 L_m, \quad V_p = \lambda^{0.5} V_m, \quad T_p = \lambda^{0.5} T_m, \quad F_p = \lambda^3 F_m \qquad (1)$$

where L = characteristic length, V = velocity, T = time, F = force, λ = scaling factor and subscripts p and m refer to prototype and model, respectively.

As in the pilot study [10], we used a JONSWAP wave energy spectrum to simulate the operating irregular seas of the platform. We set our target significant wave height as 7 m and peak period at 11.7 s (full-scale), with a peak enhancement factor of 2.2.

We fabricated two blocky bergy bit models with full-scale masses of about 1000 and 5000 tonnes. They were made of paraffin wax with a specific gravity of 0.87, which approximates that of glacial ice. The details of the two bergy bits are as follows:

	Dimension [cm]	KG[1] [cm]	Mass [kg]
Large berg	24x24x22(high)	10.71	11.58
Small berg	14x14x14	6.86	2.62

The semi-submersible model represents the NEKTON 8000 FPV, a floating oil production platform proposed by Bouygues Offshore Canada Limited for use on the Grand Banks [19]. Its large structural members (see Figure 1) are characteristic of designs being considered for oil production in ice-infested waters. Its ballast conditions are shown in Table 1.

The mooring system for the platform consisted of 12 lines arranged in the pattern being considered for the prototype (three lines extending from each corner column). Each mooring line was connected to a spring attached

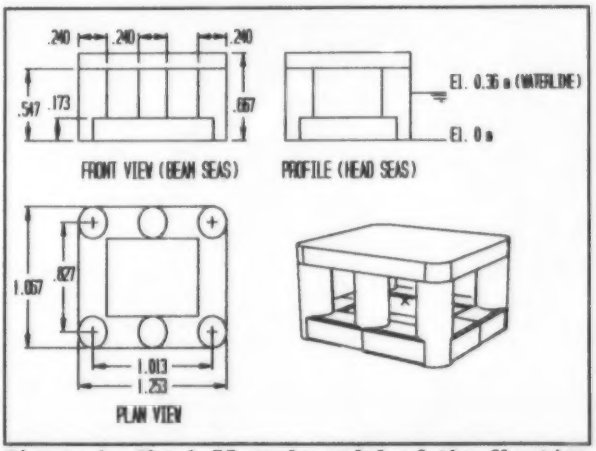

Figure 1. The 1:75 scale model of the floating production platform (All dimensions in meters).

[1] Distance from the center of gravity to the bottom face.

Table 1. Platform ballast conditions.

	Prototype	Target model	Actual model
Mass	86,779 t_3	200.68 kg_3	200.68 kg_3
Disp.	84,662 m^3	0.20068 m^3	0.20068 m^3
KG	17.542 m	0.2339 m	0.2324 m
$(GM)_{Trans}$	10.03 m	0.1337 m	0.1357 m
$(GM)_{Long}$	10.06 m	0.1341 m	0.1352 m
$(Kxx)_{roll}$	31.484 m	0.4198 m	0.4193 m
$(Kyy)_{pitch}$	35.199 m	0.4693 m	0.4671 m
Draft	27 m	0.360 m	0.357 m

to the deck of the platform. From the spring, each extended vertically down the side of a column to an underwater pulley and then to the bottom of the wave tank. We estimated the natural frequencies for head-sea surge motion and beam-sea sway motion to be 0.13 Hz and 0.16 Hz, respectively. Because these values are well below the dominant frequencies of wave energy, we did not expect the model mooring to influence the measured impacts.

The test program investigated both the open-water and impact behaviour of the models. We conducted several test series to study impact velocities and locations as a function of two berg sizes (1000 & 5000 tonnes) and two rig orientations (head & beam seas). Table 2 provides the general test conditions.

Table 2. General test conditions. (CR = Centerline of rig; FC = Front of a column; RS = Regular seas; IS = Irregular seas; OW = Open water)

Test Series	Rig Orientation	Seas	Berg Size	BergRelease Location & No. of runs
A	Head seas	IS	Large	CR (11) FC (10)
B	Head seas	IS	Small	CR (7) FC (6)
C	Beam seas	IS	Large	CR (18)
D	Beam seas	IS	Small	CR (10)
E	Head seas	RS	Large	CR (20)
F	Head seas	RS(OW)	No berg	(10)
G	Beam seas	RS(OW)	No berg	(10)
H	No rig	RS(OW)	Large	(10)
I	No rig	RS(OW)	Small	(10)

At the beginning of each impact run, we held the bergy bit at its release location, which was approximately 1.35 m upstream of the platform (see Figure 2). When the first wave approached the platform, we released the bergy bit, which then with time interacted with the platform. Throughout each run (45 seconds in duration), the following devices acquired data:

(1) a SELSPOT camera system, to record the 6 degrees-of-freedom of both the bergy bit and the platform;
(2) a video camera with a digital timer display, to record the impact sequences;
(3) 2 capacitive wave probes, to measure the wave elevation;
(4) 11 piezoelectric sensors (10 cm x 10 cm) mounted on likely impact locations of the platform, to register the impact times.

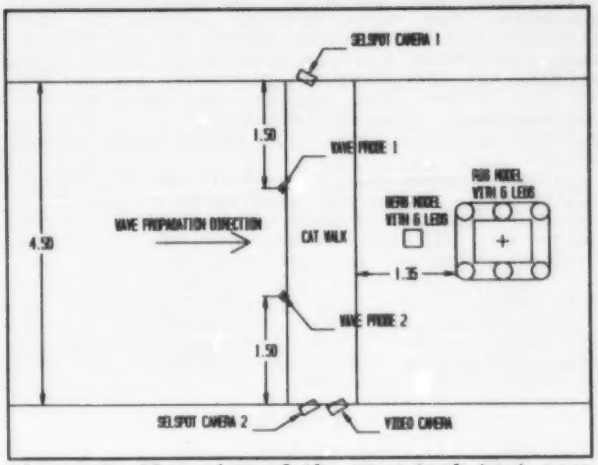

Figure 2. Plan view of the wave tank test area with the rig in the head sea orientation (All dimensions in meters).

The SELSPOT system uses two optical cameras to track 6 light emitting diodes on each model being monitored. Sequential firing of the diodes enables them to be identified and focused by the cameras. From the camera positions and line vectors to the diodes, system software calculates their space co-ordinates. From the measured positions of the diodes and their known locations on the models, the system computes the translations and rotations of the models.

At any instant, SELSPOT requires only 3 diodes to track a model. The remaining diodes on each model improve measurement accuracy via a best-fitting technique. The raw positional data were collected at a rate of 312 frames per second and then averaged over small time increments to improve signal/noise. The resulting time series records consist of the 6 degrees-of-freedom of each body sampled at 19.5 Hz.

We conducted static displacement tests to estimate the systematic and random errors in velocity calculations based on the SELSPOT data. We found that the systematic error in velocity estimates is about 5%. Based on the standard deviations of the measured positions, we estimated the maximum random error in velocity estimates based on a successive pair of displacements to be about 10%. These are well within the usual experimental error.

During data analysis, we sometimes found bergy bit displacements much larger than normal. One cause of this error is reflection of diode light off the water surface, which in turn shifts the apparent position of that diode. Very large forward rotations of the bergy bit also yield erroneous displacements due to the loss of tracking of one or more diodes. These errors were usually quite

noticeable and rendered the affected data unusable. The more limited motion of the platform and the greater height of its diodes over the water surface made this less of a problem for the platform. The wider separation of its diodes also enables better position estimations. Hence, errors in platform velocities are smaller than those of the bergy bit.

The piezoelectric sensors, which output a high voltage upon collision with a bergy bit, yielded estimates of impact times. Although the bergy bit did not always collide with the limited number of sensors used, we found that they also responded to vibration of the platform resulting from impacts. Such responses also yielded estimates of impact time. We synchronized the recording of the SELSPOT data, the video images and the piezoelectric sensors to within ± 0.2 seconds.

3.0 DATA ANALYSIS METHODOLOGY

We modified the data analysis methodology developed in the pilot program to improve processing efficiency. The basic processing steps are as described briefly below; details can be found in reference [10]. As before, we recreated the impacts using a CAD software called Integrated Design Engineering Analysis Software (IDEA-S) on a VAX 8530 computer. The software checked for contact between the bergy bit and the platform at each time step. We thus obtained estimates of impact times and locations on the rig. For quality control, we verified these CAD impact recreations against the video and piezoelectric sensor records.

We needed this quality control because, due to small position errors, the SELSPOT output might suggest a collision when there was actually a near miss. Likewise, it might predict a near miss when an impact indeed occurred. In addition, random errors might shift the impact times based on the motion recreation procedure.

To access this latter effect, we plotted the bergy bit displacements versus time near impacts and found in many cases that we could identify impact times from the measured rebound. This eliminated any inaccuracy due to time lag among different acquisition devices. Such verification was not achieved in the pilot study because of the higher noise level. Improvements in the SELSPOT system software, the redundant diodes and a two fold increase in the sampling rate combined to produce substantially better data quality than achieved in the pilot study. Even so, the extent of bergy bit rebound was sufficiently small, particularly with light impacts, that we could not use this method solely to determine the impact times.

To pass the quality control, the CAD-determined impact time had to agree with the video and piezo-electric sensor records to within ± 0.2 seconds. Also, an apparent intersection or separation between the two models had to be less than 2 cm. In addition, the general CAD-recreated model behaviour had to correspond to the behaviour recorded on video. We then examined the remaining impacts for unusual SELSPOT contamination (caused by reflection of diode light from the water surface which resulted in unrealistically large displacements): data contaminated in this way were discarded.

Using this valid data set, we calculated the impact velocities and kinetic energies. The velocity estimates were based on the backward difference of successive absolute displacements just prior to the time of impact. The linear CG velocities and mass and the rotational velocities and mass moment of inertia about the principal axes were then used to compute the translational and rotational kinetic energies respectively.

4.0 EXPERIMENTAL RESULTS

4.1 Open Water Behaviour (Series F - I)

We generated an average wave-energy spectrum using 61 wave records and found the average significant[2] wave height to be 10 m at full scale. This was higher than that of the 7 m target spectrum, but it compares well with a 10 m full-scale JONSWAP spectrum except for an increase of about 0.1 Hz in the peak frequency (see Figure 3).

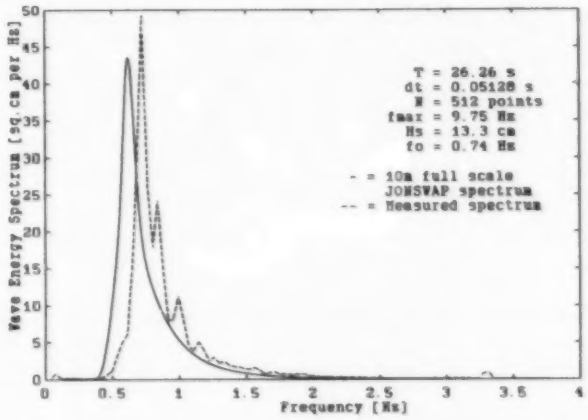
Wave Energy Spectrum [sq.cm per Hz]
Frequency [Hz]
T = 26.26 s
dt = 0.05128 s
N = 512 points
fmax = 9.75 Hz
Hs = 13.3 cm
fo = 0.74 Hz
- = 10m full scale JONSWAP spectrum
-- = Measured spectrum

Figure 3. Comparison of the 10 m full scale JONSWAP spectrum (Hs = 13.3 cm, fo = 0.62 Hz) with the average measured wave energy spectrum of 61 trails (Hs = 13.3 cm, fo = 0.74 Hz).

We acquired open-water bergy bit motion in the absence of the platform. On average, SELSPOT recorded 7 seconds of reliable data before the model drifted past the viewing area.

With the large berg, we obtained 8 valid records. With each record, we computed surge and heave displacement spectra using a Fast Fourier Transform which we then averaged. Using equations 2 and 3 given below, we then calculated the average velocity spectra and the significant velocities (e.g. [21]). Because the wave energy extended only to 2 Hz, we used a low pass filter to remove noise above this frequency.

---

[2] If N measurements are ordered in a list from the largest to the smallest, the significant is the average of the first N/3 measurements in the list. In a more physical sense, it is, roughly, an average as sensed by an observer.

$$Sv(f) = Sx(f) * (2\pi f)^2 \quad (2)$$

$$(Vx)sig = 2 * \sqrt{(m0)_v} \quad (3)$$

where Sv(f) = Velocity spectrum.
Sx(f) = Displacement spectrum.
f = Frequency.
(Vx)sig = Zero-to-peak significant velocity.
$(m0)_v$ = Zeroth moment of velocity spectrum.

The bergy bit zero-to-peak significant surge and heave velocities were found to be 2.22 m/s (2.29 m/s)[3] and 2.72 m/s (2.79 m/s)[3], respectively, at full scale. In addition, the average drift velocity was 0.44 m/s at full scale.

The curves generated by Lever et al. [20] for these conditions based on linear superposition yield significant surge and heave velocities of 2.13 m/s and 3.46 m/s, respectively, at full scale. Thus, there is reasonable agreement between the two studies. The small discrepancies could be due to errors in using linear superposition and the differences between the target and measured spectra.

With the small berg, we found that its large rotations and the close positioning of its diodes caused erroneous measurements. As a consequence, we did not conduct an analysis of its open-water behaviour.

We examined the platform's open-water behaviour in irregular waves in two ways: using its measured motion record prior to the first bergy bit impact and using linear superposition of its measured regular-wave response with the measured wave energy spectrum (e.g. [21]). We found good agreement between the motion spectra generated by the two methods, suggesting an insignificant effect of the bergy bit's wave field on the platform [22]. The spectra also confirmed that the platform's natural frequencies were well below the dominant frequency of the wave spectrum.

4.2 Irregular Wave Impact Behaviour

With SELSPOT, we obtained at impact 6 positions and 6 velocities for each body. Because of the difficulty in dealing with such a large data set, we condensed the data following the reasoning outlined by Lever et al. [10]. We initially simplified the data set by considering only motions in the vertical plane of wave propagation. Furthermore, the platform's motion was, in general, much smaller than that of the bergy bit. The exceptions to this involved only light impacts where the relative motion was small. Therefore, we focused attention on bergy bit behaviour.

In this fashion, we reduced the impact data set to the following: (a) the bergy bit CG surge and heave impact velocities, (b) the bergy bit impact translational and rotational kinetic energies, and (c) surge and heave Relative Velocity Indicators (RVI's, see equation (4) below), to evaluate whether the relative motion between the two bodies intensified or mitigated the impacts.

$$RVI = \frac{Vb - Vr}{Vb} \quad (4)$$

where Vr, Vb = surge/heave velocity of rig and berg contact point respectively.

An impact is intensified when the RVI is greater than 1 and it is mitigated when the RVI is smaller than 1. RVI's less than zero indicate that the platform is moving sufficiently quickly in the same direction as the bergy bit to prevent an impact in that direction.

As mentioned previously, Lever et al. [10] developed a simple theory for estimating the statistics of bergy bit impact velocities and kinetic energies using only open-water bergy bit motions. Equations 5 to 7 below show the respective impact probability densities based on this theory.

$$p(u|c) = \begin{cases} (u/\sigma_u^2)\exp[-u^2/(2\sigma_u^2)] & \text{for } u \geq 0 \\ 0 & \text{for } u < 0 \end{cases} \quad (5)$$

$$p(v|c) = |v|/(2\sigma_v^2)\exp[-v^2/(2\sigma_v^2)] \quad (6)$$

$$p(KE|c) = \frac{\exp\left(-\frac{KE}{M\sigma_v^2}\right) - \exp\left(-\frac{KE}{M\sigma_u^2}\right)}{M(\sigma_v^2 - \sigma_u^2)} \quad (7)$$

where $p(u|c)$, $p(v|c)$ = Probability distribution of bergy bit surge and heave velocity, respectively, given an impact has occurred.
σ_u^2, σ_v^2 = Variance of bergy bit surge and heave velocities, respectively, in open water.
u, v = Bergy bit surge and heave velocities, respectively.
$p(KE|c)$ = Probability distribution of bergy bit translational kinetic energy given an impact has occurred.
KE = Bergy bit translational kinetic energy.
M = Mass of bergy bit.

4.2.1 Head Sea, Large Bergy Bit (Series A)

For the head-sea, irregular wave impact tests, we identified a total of 72 impacts. 27 of these passed the quality control, and Table 3 shows the subsequent reduced data set.

A scatterplot of the bergy bit surge versus heave CG impact velocities shown in Table 3 indicated that the two are uncorrelated. This suggests that they are independent random variables and further implies that impact may occur at various points in the wave cycles. In the pilot study [10], Lever et al. observed this same trend.

From the table, the averages of the significant impact velocities are 2.02 m/s in surge and 1.62 m/s in heave. These represent, respectively, a 9% and a 40% reduction in comparison with the corresponding open-water velocities. In agreement with the pilot study results, this indicates that open-water velocities can yield conservative estimates of the significant impacts.

[3] Not corrected for spectrum broadness.

Table 3. Large bergy bit CG impact velocities and kinetic energies at full scale (Head sea, irregular wave impact tests)(1 - pontoon face; 2 - pontoon corner; 3 - pontoon top; and 4 - column).

IMPACT NUMBER	VELOCITY SURGE [m/s]	VELOCITY HEAVE [m/s]	KINETIC ENERGY TRANS. [MJ]	KINETIC ENERGY ROT. [MJ]	SURGE RVI	HEAVE RVI	IMPACT* LOCATION ON PLATFORM
15_2	0.543	-0.917	2.68	0.37	0.311	1.135	2
16_1	1.948	-2.381	22.00	0.00	0.740	1.184	2
16_2	0.639	-0.385	1.35	1.61	-1.206	1.139	2
16_3	1.489	0.027	5.35	1.47	1.159	0.181	2
21_2	2.121	0.716	11.70	2.10	0.907	0.444	2
21_4	2.243	0.969	14.00	0.11	0.996	-0.106	2
23_3	1.013	0.433	3.23	0.90	0.908	4.855	4
23_4	1.576	-1.212	9.37	0.38	0.871	1.373	2
24_1	2.701	-0.798	19.60	3.70	0.922	0.820	2
24_3	1.385	-2.398	18.10	1.65	0.721	0.813	2
24_4	0.776	0.719	2.61	2.06	2.503	1.764	2
25_1	0.336	-1.238	4.18	0.35	0.221	0.701	2
27_1	0.969	0.785	3.99	0.57	0.104	1.879	2
27_4	1.350	0.623	5.25	0.03	0.985	-0.624	2
28_1	0.641	-0.310	1.79	0.55	0.793	6.049	2
28_3	0.175	-0.577	1.72	0.43	0.884	3.202	2
28_4	1.818	0.685	8.92	0.06	0.880	-0.481	2
29_4	0.653	1.506	6.33	0.20	2.086	0.496	1
31_2	0.457	0.655	1.58	0.33	1.276	0.311	2
32_1	0.405	0.616	1.33	0.27	5.098	-14.59	2
32_2	1.290	-2.338	16.60	1.96	0.620	0.953	2
32_3	1.411	0.626	6.83	0.99	1.198	-4.751	2
33_1	0.782	-0.344	1.70	0.57	1.048	0.231	2
34_3	1.879	-0.729	9.68	4.40	0.855	1.309	2
35_1	0.150	0.168	0.22	0.01	1.974	2.528	2
35_2	2.424	-0.016	14.30	6.45	0.897	0.603	2
35_3	0.794	1.619	7.69	0.64	1.637	0.727	1
MEAN	1.184	-0.129	7.48	1.19			

Figure 4 shows histograms of the measured bergy bit CG surge and heave impact velocities. Also shown are the corresponding distributions predicted by the theory using equations 5 and 6. The σ_u and σ_v used in these equations were determined to be 1.15 m/s and 1.40 m/s, respectively, at full scale from the measured bergy bit velocity spectra in open water. The theory predicts reasonably well the measured surge impact velocities, including the absence

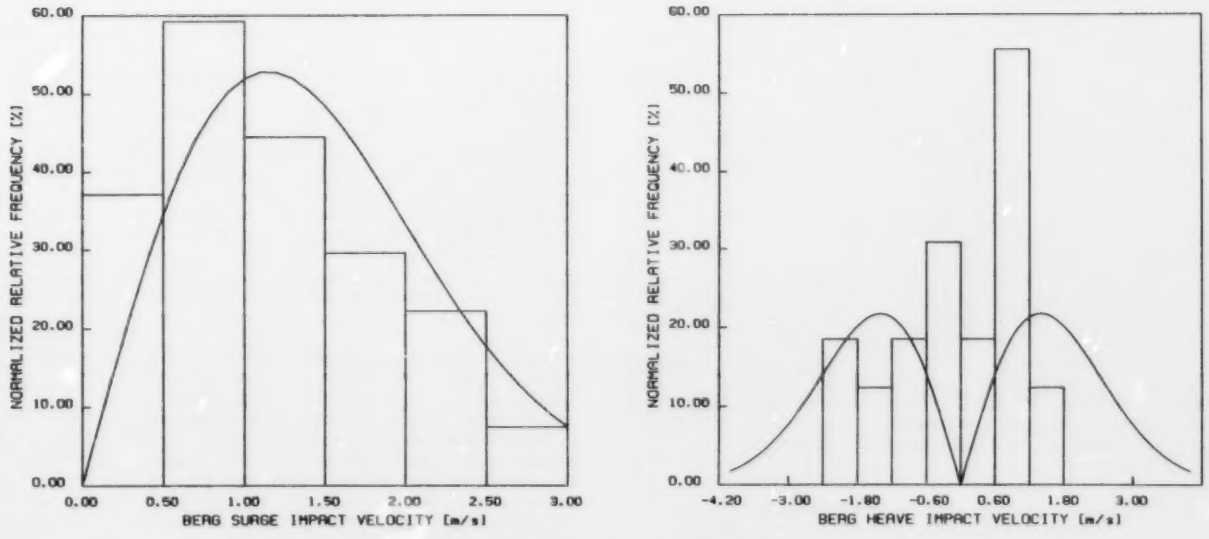

Figure 4. Histogram of the large bergy bit CG surge and heave impact velocities at full scale (Head seas).

of negative values. In heave, the predictions are not as good, with many more low velocity impacts measured than predicted.

As shown in Table 3, the mean bergy bit translation and rotational impact kinetic energies were 7.48 MJ and 1.19 MJ, respectively, at full scale. Because the rotational kinetic energy is relatively small, we considered only the statistical distribution of the translational kinetic energy.

Figure 5 compares the measured translational impact kinetic energies with distribution predicted using equation 7. Although overall the distributions agree reasonably well, the theory underestimates the number of impacts at very low kinetic energies. This is probably due to wave diffraction not accounted for by the theory because it was

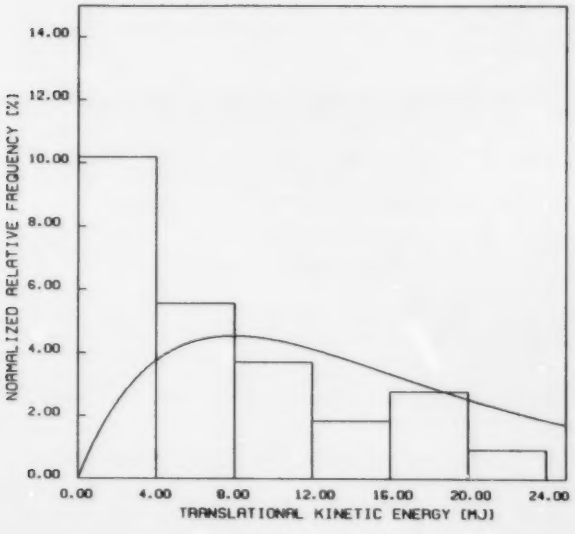

Figure 5. Histogram of the large bergy bit impact translational kinetic energies at full scale (Head seas).

developed for structures transparent to waves. The theory predicts the mean and standard deviation of bergy bit translational kinetic energy to be 16.41 MJ and 11.82 MJ respectively as compared to 7.48 MJ and 6.3 MJ obtained from the experiment. Because the simple theory ignores diffracted wave energy, it overpredicts the impact kinetic energy statistics.

With the RVI's, large values resulted whenever the berg velocities at the impact point were sufficiently small. Because small displacements are contaminated by random errors of the SELSPOT system, we omitted those RVI's outside the range of ± 2. The remaining RVI's have a mean value of 0.82 and a standard deviation of 0.58 in surge. In heave, the corresponding values are 0.71 and 0.66. This suggests that, in general, the relative motion between the two bodies has an mitigating effect on impacts. That is, treating the platform as stationary should be conservative.

4.2.2 Beam Sea; Large Bergy Bit (Series C)

For the beam sea, irregular-wave impact tests with the large bergy bit, we identified 26 impacts. The greater wave diffraction from the platform in this orientation caused fewer impacts as compared to head-sea tests. 13 of these impacts passed the quality control; Table 4 shows the resulting reduced data. Because of the small number of valid impacts, we must deal cautiously with the impact statistics.

A scatterplot of the bergy bit CG surge versus heave impact velocities again showed that they are uncorrelated. From the table, the bergy bit's full-scale significant surge and heave CG impact velocities were 1.94 m/s and 2.17 m/s, respectively. As compared to the corresponding velocities in open-water, these represent a 13% and a 20% reduction, respectively. This again shows that bergy bit open-water significant velocities are conservative estimates of impact velocities.

Figure 6 shows the distribution of the measured surge and heave CG impact velocities along with the theoretical curves obtained using equations 5 and 6. Bearing in mind the small number of impacts, the results are in reasonable agreement. However, the theory predicts no negative surge impact velocities, yet we obtained two low velocity cases. Also,

Table 4. Large bergy bit CG impact velocities and kinetic energies at full scale (Beam sea, irregular wave impact tests)(1 = pontoon face; 2 = pontoon corner; 3 = pontoon top and 4 = column).

IMPACT NUMBER	VELOCITY SURGE [m/s]	VELOCITY HEAVE [m/s]	KINETIC ENERGY TRANS. [MJ]	KINETIC ENERGY ROT. [MJ]	SURGE RVI	HEAVE RVI	IMPACT* LOCATION ON PLATFORM
80_2	2.104	2.979	31.10	0.33	1.118	0.620	4
81_1	1.134	1.004	5.51	0.12	1.089	0.976	4
81_3	1.593	-0.588	6.71	0.08	0.715	1.734	4
85_1	1.576	-0.969	8.01	0.38	1.349	1.402	2
85_2	0.723	1.887	10.50	0.40	1.062	0.801	4
88_1	0.744	-1.004	5.44	1.23	0.724	2.130	1
89_1	-0.396	-1.004	3.92	5.13	0.444	2.790	2
90_1	2.468	1.957	24.30	0.52	1.379	0.717	2
91_2	0.506	-0.900	3.02	0.44	-9.556	1.317	2
94_1	0.748	1.489	6.52	0.12	1.442	0.171	2
94_2	0.285	-1.870	8.45	0.56	-0.509	1.173	2
94_6	-0.035	0.316	0.26	0.00	-23.666	0.433	2
97_2	1.385	-0.156	7.02	2.16	1.098	1.011	1
MEAN	0.988	0.241	9.28	0.88			

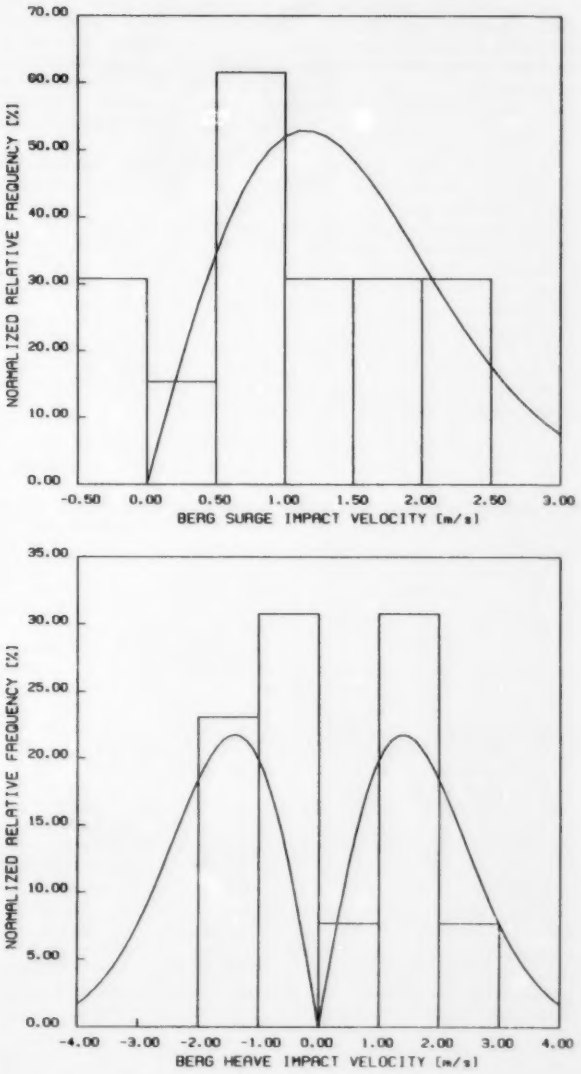

Figure 6. Histogram of the large bergy bit CG surge and heave impact velocities at full scale (Beam seas).

because a greater velocity range exists for the heave results, a close comparison with theory is difficult.

As shown in Table 4, the mean bergy bit translational and rotational impact kinetic energies were 9.3 MJ and 0.88 MJ at full scale (suggesting again that rotational impact energy is relatively small). Figure 7 compares the measured translational impact kinetic energies with the distribution predicted by equation 7. Because it ignores wave diffraction, the theory again underestimates the number of impacts at low kinetic energies. The mean and standard deviation of bergy bit translational kinetic energy obtained from the experiment were 9.29 MJ and 8.68 MJ respectively. The corresponding predicted values were 16.41 MJ and 11.82 MJ.

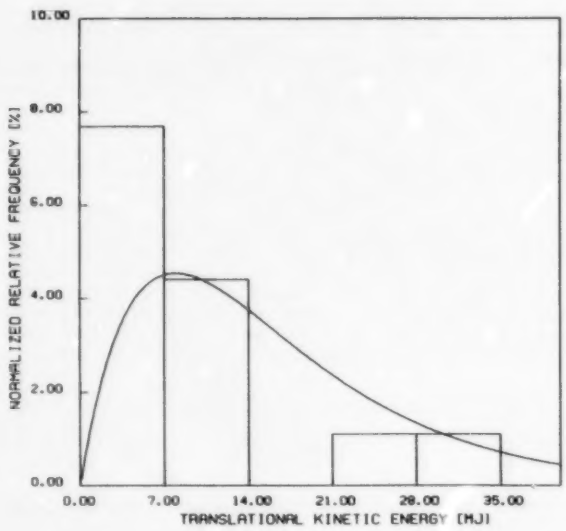

Figure 7. Histogram of the large bergy bit impact translational kinetic energies at full scale (Beam seas).

This again indicates that the theory overpredicts the kinetic energy statistics because it ignores wave diffraction.

After omitting the RVI's outside the range of ± 2, the remaining RVI's in surge have a mean value of 0.90 and a standard deviation of 0.56. The respective values in heave are 0.94 and 0.46. As with the head sea results, the platform motion tends to mitigate the impacts on average.

4.2.3 Head Sea & Beam Sea Small Bergy Bit (Series B, D)

For the small bergy bit in head seas, we identified 14 impacts. However, no impacts occurred in beam seas as a result of greater wave diffraction. We observed that diffracted waves effectively reduced the approaching velocity of the small berg, and in some beam sea tests even diverted it to the side of the platform.

The very unstable motion and large rotations of the small bergy bit caused much reflection of the diode light by the water surface. As a consequence, only three impacts passed the quality control. Because of this small number, we did not analyze the results further.

4.3 Impact Locations

With the present platform and either bergy bit model, the most likely impact location in both platform orientations was the upper corner of the pontoon that faced the oncoming waves. Even when we released the bergy bit directly in front of a column, very few impacts occurred with it because wave diffraction from the column affected the bergy bit trajectory. Diffraction sets up an annular wave system which propagates away from the column and tends to carry the bergy bit with it. It often carries it into an area where it can be driven by the incident wave into a pontoon. Consequently, a greater than expected number of impacts occurred on the pontoon. Also, waves

often threw the bergy bit onto the corner or even the top of the pontoon. As a result, impacts occurred more frequently at the corner than at the vertical face of the pontoon.

4.4 Regular Wave Impact Behaviour

Because of its broad application to vessel motion in irregular seas, it is tempting to apply linear superposition to estimate bergy bit impact statistics (e.g. [23,24]). Indeed, Lever et al. [18] showed that superposition accurately predicted iceberg open-water irregular-wave response spectra, in spite of obvious nonlinear behaviour (e.g. submergence, large excursions). However, a spectrum contains no phase information, something which could be critical for wave-driven impacts of icebergs with moving structures. Phase information in the wave system itself would be controlled by its group characteristics, as this governs the time sequencing of its components. Nonlinear phenomena such as submergence may also have a dominant effect on the phasing at impact. For example, even in regular waves, small differences in starting conditions for the two bodies in question might lead to large differences in the resultant motions of the bodies and thus in the impacts themselves.

To assess these issues, we conducted regular-wave impact tests over the frequency range of the target JONSWAP spectrum (0.4 - 1.3 Hz in 0.1 Hz increments). Because of limited tank time, we conducted only two runs at each frequency, although each run typically yielded several impacts. Table 5 shows the results which passed quality control.

It is immediately obvious that, for these tests, each run for a given wave frequency did not always generate the same number of impacts. Even when comparing first impacts (designation _1), the results for each frequency vary substantially. For some reason, the phasing of the body motions can be different from one run to the next, even in the same regular wave. One should note that we took no special precautions to minimize differences in release conditions or wave height between runs. However, we believe these were small. So, it appears that regular-wave impact results are sensitive to small differences in test conditions. This may be a reflection of the nonlinearities inherent in the phenomenon. It may also be due to small

Table 5. Large bergy bit CG impact velocities and kinetic energies at full scale (Head sea; regular wave impact tests)(1 - pontoon face; 2 - pontoon corner; 3 - pontoon top; 4 - column).

IMPACT NUMBER	VELOCITY SURGE [m/s]	VELOCITY HEAVE [m/s]	KINETIC ENERGY TRANS. [MJ]	KINETIC ENERGY ROT. [MJ]	IMPACT* LOCATION ON PLATFORM
37_1(1.3Hz)	-0.688	-0.163	1.21	1.22	1
37_5	0.517	-0.084	2.67	3.51	1
37_8	0.582	-0.206	0.89	0.06	1
112_1	0.158	-0.064	0.69	0.36	1
112_3	0.229	0.224	0.61	0.07	1
112_6	-0.190	0.018	0.12	0.62	1
112_7	0.188	-0.005	0.09	0.20	1
112_8	-0.987	0.001	2.86	0.27	1
112_9	0.006	-0.192	0.61	0.35	1
112_10	-0.592	-0.337	2.48	0.11	1
38_1(1.2Hz)	INVALID SELSPOT DATA				1
113_1	-0.430	-0.380	0.78	0.17	1
113_2	-0.400	0.010	0.89	0.30	1
39_1(1.1Hz)	NO IMPACT				
114_1	INVALID SELSPOT DATA				4
40_1(1.0Hz)	0.400	1.714	7.59	0.58	1
115_1	0.353	-0.513	1.40	0.75	1
115_2	0.800	-0.394	1.94	0.92	1
115_3	-0.433	-0.533	1.48	0.27	1
115_4	0.122	-0.013	0.98	0.35	1
115_5	-0.337	-0.581	1.84	0.16	1
115_6	-0.021	0.616	1.03	0.57	1
41_1(0.9Hz)	INVALID SELSPOT DATA				1
41_2	-0.556	-1.047	3.29	0.51	2
41_3	0.826	0.575	2.40	0.17	2
116_1	INVALID SELSPOT DATA				2
42_1(0.8Hz)	1.290	-0.185	4.46	1.56	2
42_3	0.222	-1.654	6.52	1.34	2
42_4	0.687	-1.368	5.47	0.59	2
42_5	0.535	-1.645	7.37	2.31	2
117_1	-0.094	-1.402	4.62	0.26	2
117_2	0.211	-2.156	11.00	0.53	2
117_3	0.678	-0.342	1.34	0.86	2
43_1(0.7Hz)	NO IMPACT				
118_1	0.883	-0.995	4.11	0.31	2
44_1(0.6Hz)	INVALID SELSPOT DATA				2
119_1	NO IMPACT				
BELOW 0.5Hz	NO IMPACT				

start up transients which were often still present in the rig's motion at impact. Certainly, transients generated by an impact would have an influence on subsequent impacts, if any.

We noted that at high frequencies, the berg sway motion was comparable to the surge and heave motions. As a result, the kinetic energy calculated from the three translational velocities was higher than that based just on the surge and heave velocities. At lower frequencies, where surge and heave velocities dominate, the total kinetic energy was close to that based just on the surge and heave velocities.

5.0 DISCUSSIONS & CONCLUSIONS

In the pilot study, bergy bit impacts with an oil exploration platform were considered. The present work was concerned with impacts with a production platform. Because the two studies involved similar bergy bit sizes and irregular sea states, the differences in results primarily reflect the difference in wave-making characteristics of the two structures. Although a greater number of tests would ideally generate more detailed statistical distributions, the histograms obtained nevertheless show the general trends.

We first consider similarities between the two studies. We found again that open-water bergy bit significant velocities provide conservative (10 - 40% higher) estimates of the significant impact velocities. As before, the relative motion of the two bodies at the point of contact tends to mitigate the impact slightly. Furthermore, the present results confirm two key simplifications of the theory based on the pilot study results: uncorrelated surge and heave impact velocities and small rotational kinetic energy.

In contrast to the pilot study, however, wave diffraction from the robust production platform played a much more significant role. This led to fewer impacts in beam seas than in head seas, due to greater blockage, and a substantially reduced impact rate for the 1000 tonne versus the 5000 tonne bergy bit. Furthermore, while the simple theory yielded quite good agreement with the measured impact kinetic energies for the transparent structure tested previously, here it consistently underestimated the percentage of low-energy impacts. Although this is conservative, it suggests that we could achieve closer agreement by utilizing in the theory the platform-affected, near-field bergy bit response rather than the far-field (open-water) response. We are presently considering this approach.

Lastly, our regular-wave test series revealed that significantly different impact behaviour is possible at each wave frequency. Because the wave-induced impact process is nonlinear, initial conditions and motion history will, in general, influence the impacts obtained. Thus, linear superposition may not be applicable for obtaining impact statistics.

ACKNOWLEDGEMENTS

The authors gratefully acknowledge the support and co-operation provided throughout the test program by Bouygues Offshore Canada Limited, including permission to publish the results. We also thank Mr. M. Sullivan, Mr. L. Little and Mr. Andrew Kuczora for their ceaseless efforts to upgrade the SELSPOT data quality, and Dr. D.B. Muggeridge for his continued support of our wave tank program. The authors further acknowledge the financial assistance of the Centre for Cold Ocean Resources Engineering, the Canada-Newfoundland Offshore Development Fund and the Natural Sciences and Engineering Research Council of Canada.

6.0 REFERENCES

1. Manadrill Drilling Management Inc. (1984), "An Evaluation of Ice Management Systems In Support of Eastern Canada Offshore Exploratory Drilling Operations", Royal Commission on the Ocean Ranger Marine Disaster Supporting Document, Royal Commission on the Ocean Ranger Marine Disaster, St. John's, Nfld., 54p.

2. Miller, J.D., (1982), "Tactical Iceberg Management III - Collision Avoidance", Seminar on Iceberg Management in Offshore Exploration, Production and Transportation, St. John's, Nfld., pp. 81-102.

3. Lever, J.H., Reimer, E. & Diemand, D. (1984), "A Model Study of the Wave Induced Motion of Small Icebergs and Bergy Bits", 3rd International Symposium on Offshore Mechanics and Arctic Engineering, Vol. 3, pp. 282-290.

4. Curtis, D.D., Cammaert, A.B., Wong, T.T. & Bobby, W. (1984), "Numerical Analysis of Impact of Small Icebergs on Semi-submersibles", Proc. of Cold Regions Eng. Spec. Conf., Edmonton, Alberta. pp. 415-430.

5. Swamidas, A.S.J., El-Tahan, H., & Arockiasamy, M. (1986), "Structural Integrity of Semi-submersibles & Gravity Platforms to Bergy Bit/Iceberg Impact", 18th Technology Conference, paper 5087, pp. 39-49.

6. El-Tahan, H., Arockiasamy, M. & Swamidas, A.S.J. (1986), "Motion & Structural Response of a Hydro-elastic Semi-submersible Model to Waves & Ice Impacts", Proc. of IV International Symposium on Offshore Mechanics & Arctic Engineering, Dallas, Texas, pp. 753-761.

7. Kitami, E., Fujishima, K., Taguchi, Y., Nawata, T., Kawasake, T., & Sakai, F. (1984), "Iceberg Collision with Semi-submersible Drilling Unit", Proc. of IAHR Ice Symp., Hamburg, W.G., pp. 45-53.

8. Anderson, K.G., McDonald, D., Mitten, P., Nicholls, S. & Tait, D. (1986), "Management of Small Ice Masses", Environmental Studies Revolving Funds, Report No. 042, Ottawa, 195p.

9. Borthwick, I. & Hadley, R.D. (1985), "Ice and Iceberg Contingency Planning & Management for Offshore Oil and Gas Operations", Proceedings of POLARTECH'86, Helsinki, Finland, Vol. 1, pp. 323-339.

10. Lever, J.H., Colbourne, B., Mak, L. (1989), "Model Study of the Wave-driven Impact of Bergy Bits with a Semi-submersible", 8th International Conference on Offshore Mechanics & Arctic Engineering, The Hague, Netherlands, Vol. 4, pp. 393-403.

11. Isaacson, M. & Dello Stritto, F.J. (1986a), "Motion of an Ice Mass Near a Large Offshore Structure", 18th Offshore Technology Conference, Houston, paper 5085, pp. 21-28.

12. Isaacson, M. (1986b), "Ice Mass Motions Near an Offshore Structure", Proc. 5th Offshore Mechanics & Arctic Engineering Symposium, Tokyo, Vol. 1, pp. 441-447.

13. Salvalaggio, M.A. & Rojansky, M. (1986), "The Importance of Wave Driven Icebergs Impacting an Offshore Structure", 18th Offshore Technology Conference, Houston, paper 5086, pp. 29-38

14. Pawlowski, J.S. & Wishahy, M.A. (1987), "Time Domain Simulation of the Drifting of Small Floating Bodies in Waves", 9th Int. Conf. on Port and Ocean Engineering Under Arctic Conditions, Fairbank, Vol. 1, pp. 239-251.

15. Wishahy, M.A., Pawlowski, J. & Muggeridge, D. (1987), "The Nonlinear Heave Motion & Wave Forces on a Partially Submerged Sphere", Proceedings of Oceans'87, Vol. 1, pp. 42-47.

16. Nessim, M.A., Murray, A., Maes M.A. and Jordaan, I.J. (1984), "Risk Analysis Methodology for Mobile Offshore Units Operating in Ice-infested Waters", Ice Tech'84, 3rd Int. Conf. on Icebreaking and Related Technologies, SNAME, pp. H1-H12.

17. Jordaan, I.J. (1987), "Probabilistic Analysis of Environmental Data for Design of Fixed and Mobile Arctic Offshore Structures", 5th Int. Conf. on Applications of Statistics and Probability in Soil and Structural Engineering (ICASP), Vancouver.

18. Lever, J.H., Attwood, D. & Sen, D. (1988a), "Factors Affecting the Prediction of Wave Induced Iceberg Motion", Cold Regions Science and Technology, Vol.15, pp.177-190.

19. Valenchon, C.P., Jardinier, R.C., Sparks, C.P. and Manesse, J.P. (1987), "The Concrete Floating Production Platform 'NEKTON 8000'", 6th International Symposium on OMAE, Houston.

20. Lever, J.H., Sen, D. and Attwood, D. (1988b), "The Influence of Shape on Iceberg Wave-induced Velocity Statistics", 7th Int. Conf on OMAE, Houston, Vol. 4, pp. 125-132.

21. Bhattacharyya, R. (1978), "Dynamics of Marine Vehicles", Wiley, New York.

22. Mak, L.M. (1989), "An Experimental Study of Wave Induced Impacts of Bergy Bits with a Floating Production Platform", M. Eng Thesis, Faculty of Engineering and Applied Science, Memorial University of Newfoundland, St. John's, Newfoundland.

23. Lindberg, K. & Andersson (1987), "Ice Impacts on Semi-submersibles", 6th Offshore Mechanics and Arctic Engineering Symposium, Houston, Vol. 4, pp. 313-320.

24. Andersson, L., Lindberg, K. & Ygge, A. (1986), "Structural Safety of Semis in Sub-arctic Waters", Polartech '86, Helsinki, Vol.2, pp. 540-555.